

Article

MPPT for a PV Grid-Connected System to Improve Efficiency under Partial Shading Conditions

Abdulaziz Almutairi ¹, Ahmed G. Abo-Khalil ^{1,2,*} , Khairy Sayed ³ and Naif Albagami ¹

¹ Department of Electrical Engineering, College of Engineering, Majmaah University, Almajmaah 11952, Saudi Arabia; ad.almutiri@mu.edu.sa (A.A.); n.albagami@mu.edu.sa (N.A.)

² Department of Electrical Engineering, College of Engineering, Assuit University, Assuit 71515, Egypt

³ Electrical Engineering Department, Faculty of Engineering, Sohag University, Sohag 82524, Egypt; khairy_sayed@eng.sohag.edu.eg

* Correspondence: a.abokhalil@mu.edu.sa

Received: 13 November 2020; Accepted: 8 December 2020; Published: 10 December 2020



Abstract: The disadvantage of photovoltaic (PV) power generation is that output power decreases due to the presence of clouds or shade. Moreover, it can only be used when the sun is shining. Consequently, there is a need for further active research into the maximum power point tracking (MPPT) technique, which can maximize the power of solar cells. When the solar cell array is partially shaded due to the influence of clouds or buildings, the solar cell characteristic has a number of local maximum power points (LMPPs). Conventional MPPT techniques do not follow the actual maximum power point, namely, the global maximum power point (GMPP), but stay in the LMPP. Therefore, an analysis of the occurrence of multiple LMPPs due to partial shading, as well as a study on the MPPT technique that can trace GMPP, is needed. In order to overcome this obstacle, the grey wolf optimization (GWO) method is proposed in order to track the global maximum power point and to maximize the energy extraction of the PV system. In addition, opposition-based learning is integrated with the GWO to accelerate the MPPT search process and to reduce convergence time. Simultaneously, the DC link voltage is controlled to reduce sudden variations in voltage in the event of transients of solar radiation and/or temperature. Experimental tests are presented to validate the effectiveness of the proposed MPPT method during uniform irradiance and partial shading conditions. The proposed method is compared with the perturbation and observation method.

Keywords: photovoltaic; grey wolf optimization; global maximum power point

1. Introduction

In the last few decades, increased demand for electricity has made the search for the use of renewable energy sources increasingly necessary, attracting strong interest in the diversification of power generation plants. In addition, considering the increasing interest in clean and sustainable energy and the reduction of the impact on the environment, the use of renewable energy sources has been prominent, mainly because these energy sources are the main contenders to replace polluting fossil-based energy systems.

In this context, wind and solar energy reached prominence among the various sources of renewable energy for the production of electricity from distributed energy generation systems (DGs). To be specific, the production of energy from solar energy, using photovoltaic cells, has become indispensable for the strengthening of DG systems [1–5].

Photovoltaic (PV) modules are responsible for converting solar energy into electrical energy. These modules are composed of several interconnected PV cells to provide a voltage and electric current value that can be used in practice, as well as form a set that provides adequate protection for the cells.

Karami et al. [6] have shown that the energy conversion efficiency of the best solar cells, which are laboratory manufactured and made of monocrystalline silicon, is of the order of 25%, which represents a low value when a comparison is made with other currently used forms of energy generation.

Another important point to be considered is that the voltage and output current of the PV modules also vary according to environmental conditions such as temperature and the incidence of solar radiation. In order to extract the maximum power from the module in the existence of these variables, DC-DC converters are used with algorithms for tracking the maximum power point (MPPT) [7].

The evolution of research in the development of new algorithms for searching MPP resulted in increased efficiency and the better use of energy generation throughout the day. Therefore, in addition to providing energy to the grid, the search for the extraction of maximum power from PV arrangements has been one of the main challenges to be addressed in the implementation of PV systems. To this end, techniques have been systematically used to track the MPP [8]. In contrast, the effects caused by partial shading can affect the maximization of energy produced from PV systems. Thus, to solve this problem, control strategies as well as converter topologies have been adopted in most applications of PV systems connected to the network. MPPT techniques can be classified into four categories [9–26]:

1. Model-based methods:

- Constant voltage
- Constant current
- Pilot cell
- Curve fitting
- Look up table
- Bisect search theorem
- Best fixed voltage
- Temperature parametric
- Linear reoriented coordinates method
- Analytical solution (AS) based method
- Gradient descent

2. Heuristics methods:

- Perturbation and observation (P&O)
- Modified P&O
- Incremental conductance (IC)
- Modified IC
- Hill climbing (HC)
- Modified HC
- Comparison of three points with weighting
- Parasitic capacitance (PC) method
- Load current or voltage maximization (LCVM) method
- DP/dV or dP/dI feedback control
- Ripple correlation control
- Variable inductance
- Temperature parametric
- Beta (β) method
- Current sweep
- System oscillations
- PV output Senseless (POS)

3. Intelligent prediction-based methods:

- Fuzzy logic control
- Artificial neural network (ANN)
- Adaptive neuro-fuzzy inference system ANFIS
- Particle swarm optimization (PSO) method

4. Hybrid methods.

One of the model-based, or what is sometimes called fixed-step, methods is the open circuit voltage fraction method, which estimates the maximum power point value using the V_{oc} value as a basis, considering it to be linearly proportional to V_{max} , which is equal at a fraction of the V_{oc} value. This method, which is very simple to implement, requires a voltage sensor to be installed. However, the maximum power value is never reached because it is an estimated PV system that is constantly turned off to read the current value of V_{oc} .

The literature also identifies several modifications among the model-based techniques for improving the performance of MPPT methods by using the search-based methods that are based on perturbing strategies, such as perturb and observe (P&O) [7–9] or incremental conductance (IC) [10,11]. These methods do not require any knowledge of the PV open circuit voltage or short circuit current, which makes them flexible for application in any PV system. However, there are some important considerations regarding their operation. When subjected to continuous and rapid variations in irradiance or partial shading conditions, these algorithms may fail the maximum point of operation due to a fall in the local maximum power point.

Intelligent training-based algorithms, such as fuzzy logic or artificial neural networks, were also developed in order to increase the performance of the search for the maximum power point. Smart controllers, such as the fuzzy logic controller, showed some advantages over the P&O controller [12,13]. In addition, the neuro-fuzzy hybrid intelligent control system also showed some advantages over the P&O method [14]. Moreover, several methods of training artificial neural networks have been developed in order to improve the search speed for the point of maximum power. The maximum power point search method, P&O, was used to train a neural network, generating an optimal increasing or decreasing duty ratio in the direction of the maximum power point [15–17].

Although typical MPPT algorithm methods perform well considering the uniformly irradiated PV arrangement, their performance can be strongly affected when they operate under partial shading conditions. This is due to the fact that, in most cases, the MPPT techniques mentioned above only reach the local maximum power point (LMPP) instead of the global maximum power point (GMPP) [18].

Due to these limitations, bioinspired optimization algorithms are being used to deal with partial shading problems in the search for MPP. As a result, the efficiency of MPPT techniques has decreased. Therefore, in order to find the GMPP, MPPT algorithms based on meta-heuristic optimization methods have been proposed in the literature [18]. These methods include particle swarm optimization (PSO) [19], which is attractive due to the compromise between performance and complexity, as well as maturity in relation to optimization methods that implement totally numerical or heuristic procedures [20,21]. Thus, unlike traditional MPPT techniques that, in most cases, achieve the LMPP, the BAT-based MPPT method is able to minimize the effects caused by partial shading, due to the fact that it always reaches the GMPP, hence improving the performance of the PV system [22,23].

In contrast, it was observed in [24] that combining P&O and the Ant Colony Optimization method converges faster with the GMPP and presents lower fluctuations in steady state when compared to similar algorithms based on the PSO algorithm.

In this sense, the development of new algorithms for optimization in solving partial shading and LMPP is needed. In order to select one of the previously stated MPPT algorithms, it is necessary to configure the PV system to be able to make a comparison between the MPPT techniques [25,26]. In addition, for the techniques to work properly, it is necessary that some requirements are met:

- 1- Stability: the response of the system should be as reliable as possible and a change in energy should be correctly detected.
- 2- Fast dynamic response: it is necessary that the MPPT control responds quickly to rapid irradiance changes in order to maximize the efficiency of the PV system.
- 3- Small steady-state error: for any MPPT method, after reaching the MPP, it is impossible to maintain the tracker at a fixed point. Therefore, it is important for the system to continue running to search that point and minimize the steady-state error.
- 4- Robustness: it is important to design an MPPT control system that is robust in the face of any disturbance, such as input noise, measurement error, or variation of system parameters.
- 5- Efficiency: it is important to have an MPPT control system that performs well, with the same efficiency, in both low irradiance and high irradiance conditions. Several MPPTs have low efficiency at low irradiance levels since the controller parameters are designed for rated power and high irradiance levels.

Thus, the main contribution of this work consists of presenting, through analytical and experimental results, a PV system with a double stage of energy conversion using the MPPT technique based on the GWO method to achieve GMPP when the PV is subjected to constant solar irradiance and partial shading conditions. Opposition-based learning is used with GWO to accelerate the convergence speed of the GWO method. The implemented opposition-based learning grey wolf optimization (OGWO-MPPT) technique is evaluated through experiments and compared with the P&O method.

2. PV Model

The equivalent circuit of the PV when light is irradiated is depicted in Figure 1. Parallel resistance R_{sh} represents the leakage resistance represented by a constant resistance, which is beyond the ideal diode characteristics [25]. Since the relationship between the PV voltage and the current is severely nonlinear, modeling of the PV must be preceded in order to perform a full system simulation that can achieve accurate system characteristics.

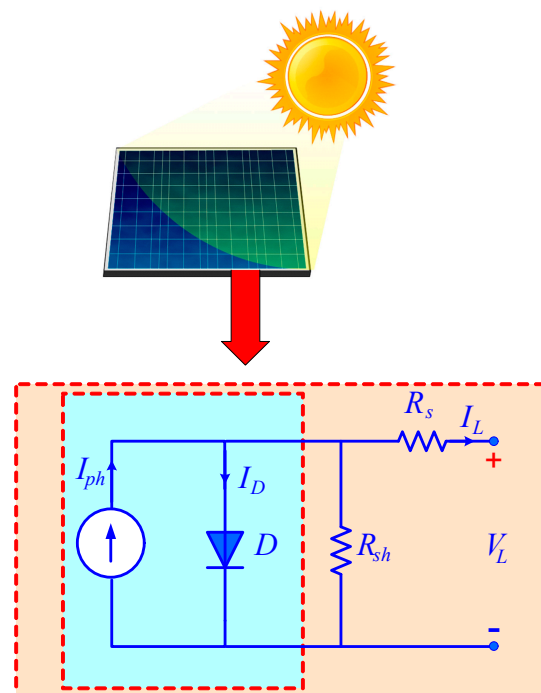


Figure 1. Photovoltaic (PV) equivalent circuit.

In a PV array, the open circuit voltage and short circuit current are given by the number of series and parallel cells

$$V_{OC} = N_s V_{oc} \quad (1)$$

$$I_{SC} = N_p I_{sc} \quad (2)$$

The PV I-V and P-V characteristics of the PV is obtained as follows [26,27]:

$$I_{ph} = I_{sc} S_N + I_t (T_c - T_r) \quad (3)$$

$$I_d = I_o \left[\exp \left(\frac{q(V_L + I_L R_s)}{A k T} \right) - 1 \right] \quad (4)$$

$$I_o = I_{or} \left[\frac{T_c}{T_r} \right] \cdot \exp \left(\frac{q E_g}{B k} \left(\frac{1}{T_r} - \frac{1}{T_c} \right) \right) \quad (5)$$

$$I_L = I_{ph} - I_d - \frac{V_L + I_L R_s}{R_{sh}} \quad (6)$$

Equation (3) is valid for a certain irradiation level S_N and at a particular operating cell temperature T_c . The I-V and P-V characteristics for various irradiation levels at a constant cell temperature can be obtained by measuring the PV, current, voltage, and power, as shown in Figure 2.

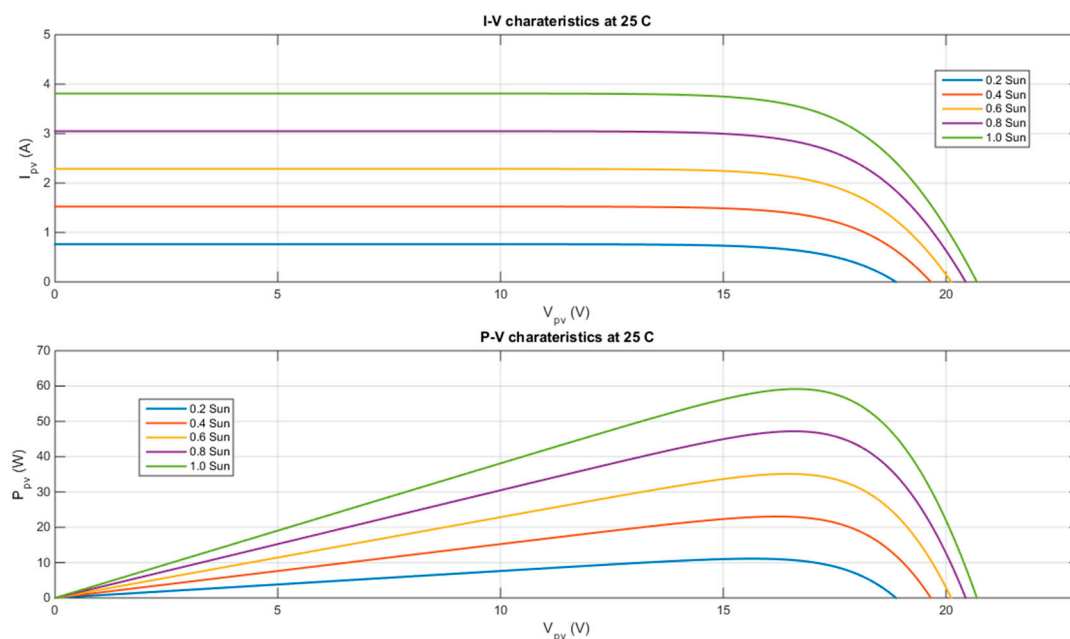


Figure 2. Voltage-current and power-current characteristics at various irradiation levels and a constant temperature.

As the irradiance and the temperature vary throughout the day, the power, the voltage, and the current also vary as a consequence. Figures 2 and 3 show the I-V and P-V with irradiance variation, respectively.

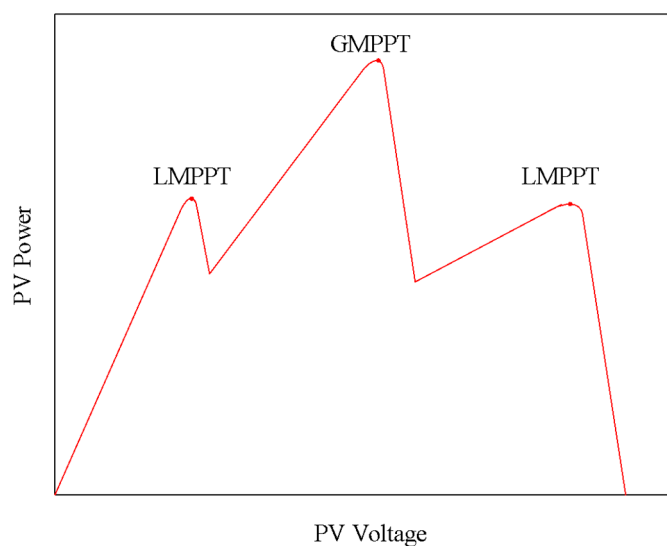


Figure 3. PV characteristics under partial shading.

3. Maximum Power Operation of Partial Shading Systems

In PV systems installed in an urban environment, it is common for the installation to suffer some shading due to the presence of obstacles in the vicinity of the installation. The impact that shading can cause will depend on various factors, including the type of PV module, the configuration of the bypass diodes, the configuration of the string, and the nature of the shadow. In the case of partial shading of the module, the power loss may be proportionally greater than the shaded area and, in addition to the loss of energy due to shading, there will be loss due to a mismatch of the electrical current between the modules of the same string as well as a loss due to the mismatch of the electrical voltage in parallel strings within the same array [28].

In order to minimize the impact on power generation of shadowing in a PV system, the modules have bypass diodes which, when polarized, deflect the current from that substring. The bypass diode works as follows: if a cell is shaded, its electrical current is reduced, and the cell's current is compatible with the substring current, that cell must be reversely polarized (acting as a charge). If the total voltage of the substring is less than zero, the bypass diode will polarize, causing the cell to operate close to the voltage. The current versus the voltage curve of a photovoltaic array will be the result of the individual curves of each substring and the series-parallel configuration of the strings.

When the system is subjected to a partial shading condition, the global maximum power point tracking action of the converter, known as GMPPT, seeks to find the value maximum global energy generation from among the several I-V curves of the module, resulting from the different conditions of partial shading. The optimization process will then seek to adjust the operation of the DC-DC converter so that it delivers the maximum output power, regardless of the partial shading condition. An example of the result of this action is shown in Figure 3 [29].

Regardless of the partial shading condition of the PV system, it is essential that the chosen timing method leads the operation of the DC-DC converter to the GMPP with agility and precision, thus guaranteeing the delivery of maximum power generated at any time and under any irradiance condition [30].

4. MPPT Using the OGWO Method

The grey wolf algorithm, which is a meta-heuristic based on the movement used by wolves when approaching prey, is hierarchically subdivided by four types of wolf: Alpha α ; Beta β ; Delta δ ; and Omega ω . This movement is divided into three stages: search for prey; attack; and capture. The adaptation of the movement to the optimization algorithm follows the wolf hierarchy, which takes the shape of a pyramid, as shown in Figure 4 [30].

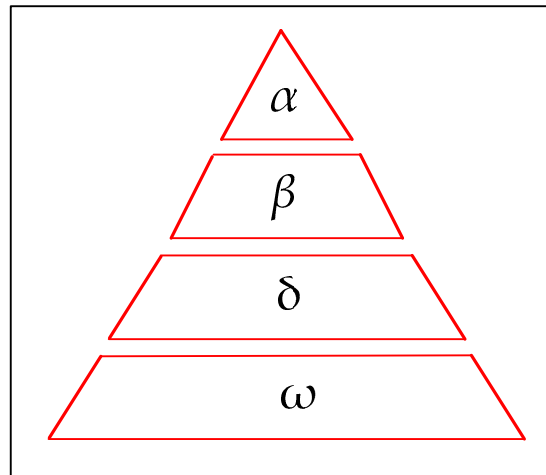


Figure 4. Hierarchy of grey wolves [30].

The social hierarchy of wolves, as discussed above, is based primarily on their level of dominance. The fitness of wolves also depends on dominant behavior, as the wolf with greater aptitude will present better performance and ability to make decisions during the hunting process. Therefore, the wolf that is in the first hierarchy level (α) is considered the fittest amongst the pack. The hunting process is performed in specific behaviors, mathematically modeled as follows [31]:

4.1. Surrounding the Prey

During the hunting process, wolves surround the prey, formulated as

$$\vec{D} = |\vec{C} \cdot \vec{X}_p(t) - \vec{X}(t)| \tag{7}$$

$$\vec{X}(t + 1) = \vec{X}_p(t) - \vec{A} \cdot \vec{D} \tag{8}$$

where t is the current iteration, \vec{A} and \vec{C} are vector coefficients, \vec{X}_p is the prey position vector, and \vec{X} is the grey wolf position vector.

The vectors \vec{A} and \vec{C} are calculated as follows:

$$\vec{A} = 2\vec{a} \cdot \vec{r}_1 - \vec{a} \tag{9}$$

$$\vec{C} = 2 \cdot \vec{r}_2 \tag{10}$$

where a decays from 2 to 0 during the iterations \vec{r}_1 and \vec{r}_2 and is a vector of random values in the interval [0–1].

4.2. Hunting for Prey

The behavior of grey wolves consists of recognizing the location of the prey and surrounding it.

However, there is no way to be sure of the prey’s exact location. To simulate this behavior, alphas, betas, and deltas are supposed to have the best knowledge of the possible prey location. The best three are then chosen, and the rest are forced to follow them. The modeling of this behavior is proposed below:

$$\vec{D}\alpha = |\vec{C}1 \cdot \vec{X}\alpha - \vec{X}|, \vec{D}\beta = |\vec{C}2 \cdot \vec{X}\beta - \vec{X}|, \vec{D}\delta = |\vec{C}3 \cdot \vec{X}\delta - \vec{X}| \tag{11}$$

$$\vec{X}1 = \vec{X}\alpha - \vec{A}1 \cdot (\vec{D}\alpha), \vec{X}2 = \vec{X}\beta - \vec{A}2 \cdot (\vec{D}\beta), \vec{X}3 = \vec{X}\delta - \vec{A}3 \cdot (\vec{D}\delta) \tag{12}$$

$$\vec{X}(t+1) = \frac{\vec{X}_1 + \vec{X}_2 + \vec{X}_3}{3} \quad (13)$$

4.3. Attacking the Prey

The grey wolves first corner the prey. When it loses its energy and stops moving, the leader closest in proximity preys on it. The vector coefficient is decreased to reduce the distance between the position of the prey and the position of the wolves. In order to reduce the distance, the value of α should be minimized as follows:

$$a = 2 - \left(\frac{2}{\text{max.iter}} \right) \quad (14)$$

where *max.iter* is the maximum number of iterations adopted in the simulation and a is decreased from 2 to 0. Figure 4 shows the displacements of the wolves in two-dimensional and three-dimensional spaces.

For tracking the MPP, the duty ratio (D) of the Boost converter refers to the positions of the wolves in each state (\vec{X}) as follows:

$$D(k+1) = D(k) - a \cdot e \quad (15)$$

The objective function of the algorithm is determined by

$$P_{pv}(k) > P_{pv}(k-1) \quad (16)$$

where $P_{PV}(k)$ is the current power, $P_{PV}(k-1)$ is the previous power at the output of the PV array, and k is the iteration value. Figure 5 shows the flowchart for the GWO method, where $P_{best,i}$ indicates the best value obtained in iteration i while G_{best} indicates the best global value found by the method.

However, the opposition-based learning (OBL) method can direct the search for the best solution by bioinspired algorithms, in the opposite direction of the current search. The process involves that, at a given moment, the agents are together around the best position found, with a decrease in diversity. In this case, this technique allows for a change of positions of some of its agents to the opposite coordinates, exploring new possibilities in the search space [32,33]. Figure 5 presents the flowchart of the opposition-based learning grey wolf algorithm (OGWO).

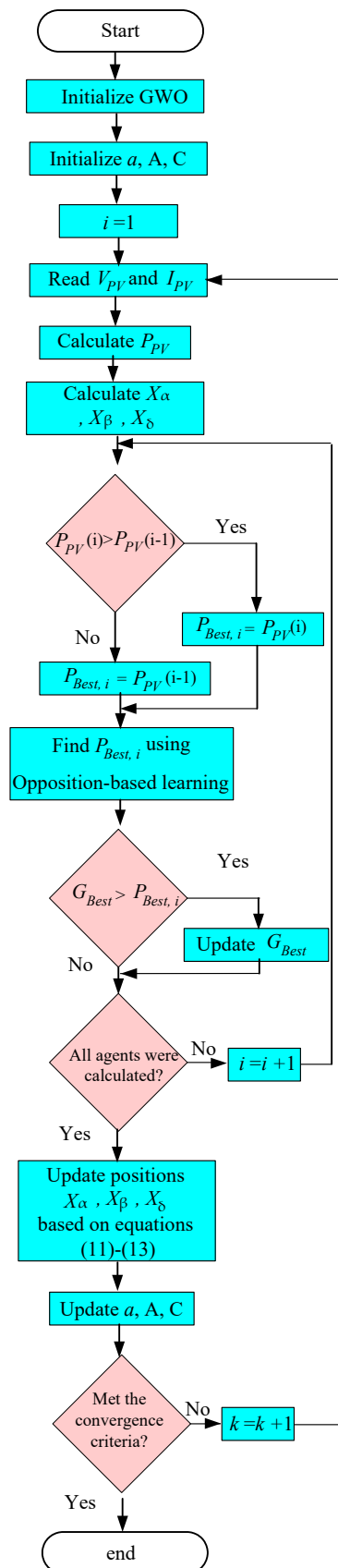


Figure 5. Flowchart of opposition-based learning grey wolf optimization (OGWO) for maximum power point tracking (MPPT).

5. System Description

Figure 6 shows the complete scheme of the PV system connected to the single-phase electrical network studied in this work. The topology consists of a PV array, followed by a DC-DC boost converter and a single-phase full bridge inverter for connection to the grid. The experimental set that is implemented is based on a digital signal processor, where all the algorithms, such as phase locked loop (PLL) and MPPT, and controllers, are embedded, as well as the current controller, inverter, boost converter MPPT controller, and inverter DC bus controller.

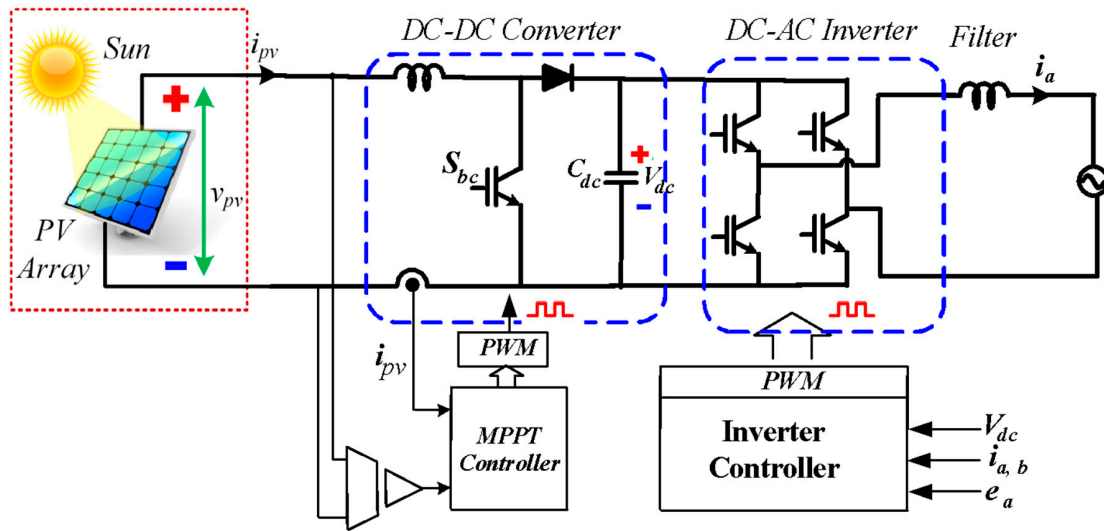


Figure 6. PV grid-connected system.

In the grid-connected inverter, DC link voltage control and output stage current control are performed. The controller of the conventional boost converter is controlled to follow the voltage reference signal (v_{pv}^*) generated as a result of the MPPT algorithm. The switch is controlled by a gating signal of a current controller, as shown in Figure 7a.

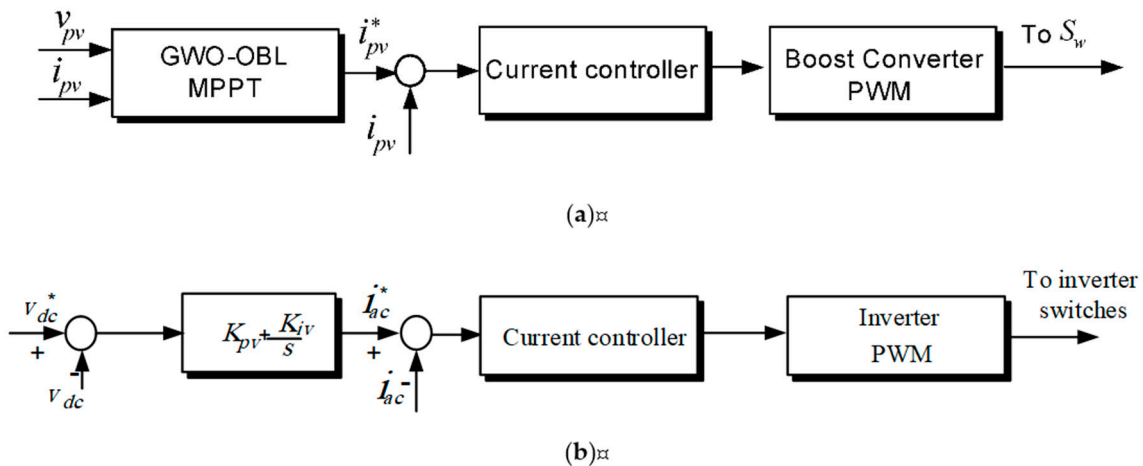


Figure 7. Control circuit for (a) the boost converter, (b) the DC-AC inverter.

The inverter, which converts the DC to the AC current that flows into the utility or local loads, also synchronizes the output current with the grid voltage and controls the DC-link voltage. Figure 7b shows the block diagram for controlling the inverter, which includes an inner loop for current control and an outer loop for voltage control. One of the important functions of the inverter is to synchronize the output current with the grid voltage to maintain a unity power and control the DC-link voltage.

6. Experimental Results

In order to validate the performance of the proposed OGWO-MPPT algorithm, an experimental setup is implemented using PV arrays, for which the specification is described in Table 1. The power circuit consists of a DC-DC converter and DC-AC inverter that are made up of insulated-gate bipolar transistor (IGBT) modules from Semikron. Through a signal conditioning circuit employing Hall effect transducers (LEM), the magnitudes of voltage and current are measured and conditioned. The MPPT and PLL algorithms and the current and voltage controllers are on the DSpace (Microlabbox). The photovoltaic arrangement consists of 60 W PV arrays with a specification as described in Table 1, while the system parameters are listed in Table 2. The experimental setup is shown in Figure 8.

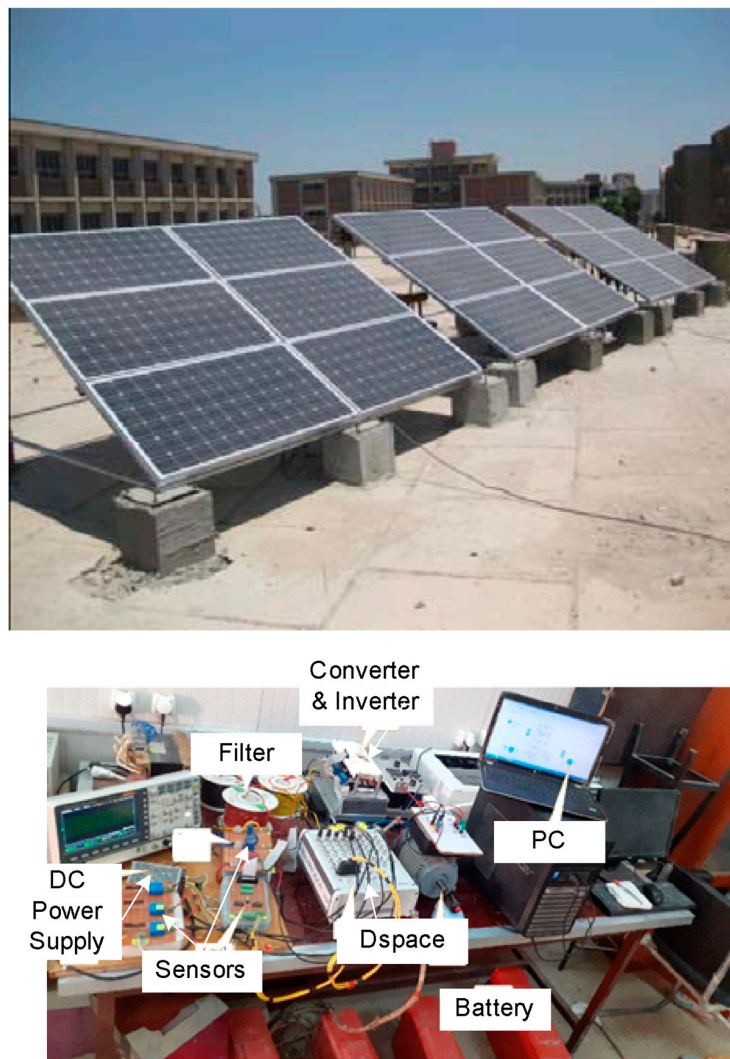


Figure 8. PV system setup.

Table 1. Parameters of the 60-W Array at 25 °C and 1000 W/m².

Maximum power	60 W
MPP voltage (V_{mp})	17.2 V
MPP current (I_{mp})	3.5 A
Open-circuit voltage (V_{oc})	21.5 V
Short-circuit current (I_{sc})	3.85 A

Table 2. System Parameters.

Grid voltage	220 V
Grid frequency	60 Hz
Filter inductance	3 mH
DC = link capacitor	330 μ F

Figure 9 shows the power extracted from the photovoltaic system using the OGWO-MPPT method when the PV array is fully exposed to the sun. Figure 9a,b show the PV voltage and current when the irradiance changes from zero to 1000 W/m². Figure 9c shows the tracking of MPP, where it took 0.5 s to achieve the maximum power point due to the effect of opposition-based learning in achieving the maximum power point faster than the regular GWO.

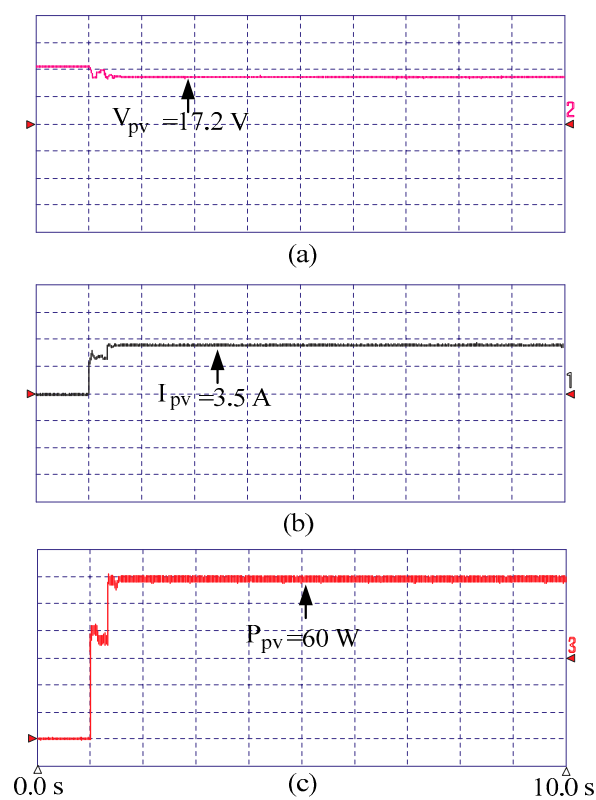


Figure 9. Maximum power point tracking time using the OGWO algorithm when irradiance increases (a) PV voltage, (b) PV current, (c) PV power.

The PV array is then partially covered by semi-transparent sheets to simulate and form a partial shading condition. The performance of the OGWO-MPPT algorithm is fast, capturing the GMMPT in less than 1 s, as shown in Figure 10. The PV voltage, current, and power are shown in Figure 10a–c.

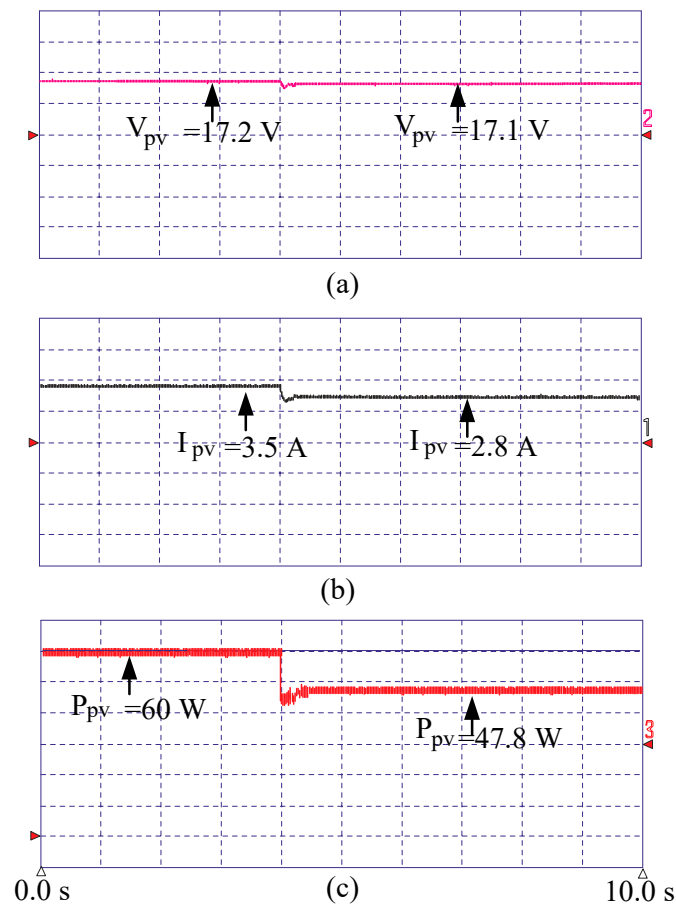


Figure 10. PV voltage, current, and power of the proposed MPPT for a different irradiation level decreases (a) PV voltage, (b) PV current, (c) PV power.

To test the OGWO-MPPT under different irradiance conditions, more semi-transparent sheets were added to cover a wider area of PV array. The tracker very quickly captured the GMPPT, still with a convergence time of less than 1 s. The PV voltage, current, and power are shown in Figure 11a–c.

In order to validate the OGWO-MPPT under different conditions, the semi-transparent sheets were removed from the PV array. The tracker very quickly captured the GMPPT, still with a convergence time of less than 1 s. The PV voltage, current, and power are shown in Figure 12a–c. The PV voltages and currents in this method are well regulated to extract the maximum power with minimum low-frequency ripples.

Figure 13 shows the PV power, current, and voltage when the P&O MPPT method is used for the same condition as Figure 11. It is obvious that P&O method has high oscillations in the steady state and take longer to reach steady state. P&O tracked an LMPP of 36 W with high oscillations around the maximum point, as shown in Figure 13c.

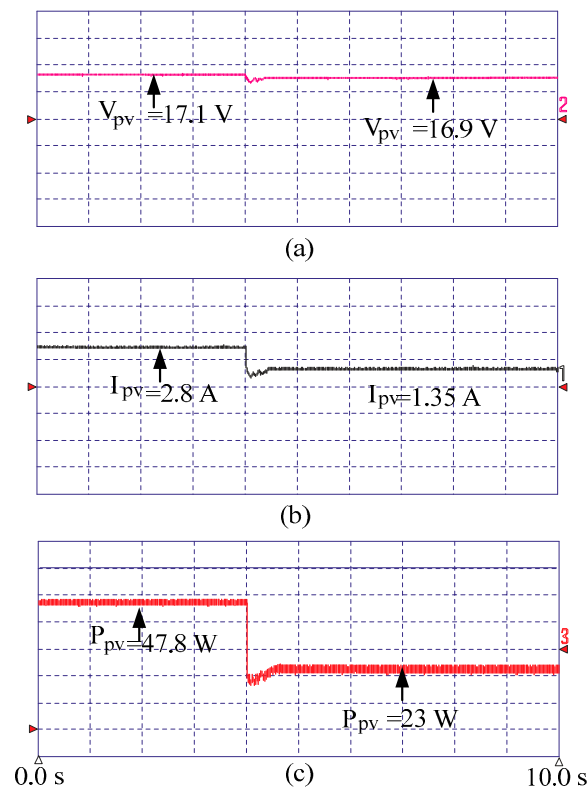


Figure 11. PV voltage, current, and power of the proposed MPPT for a different irradiation level (a) PV voltage, (b) PV current, (c) PV power.

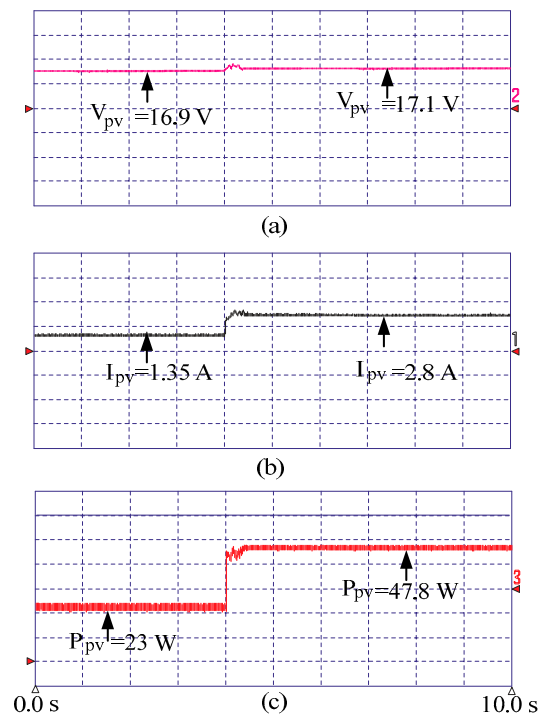


Figure 12. PV voltage, current, and power of the proposed MPPT when irradiation increases (a) PV voltage, (b) PV current, (c) PV power.

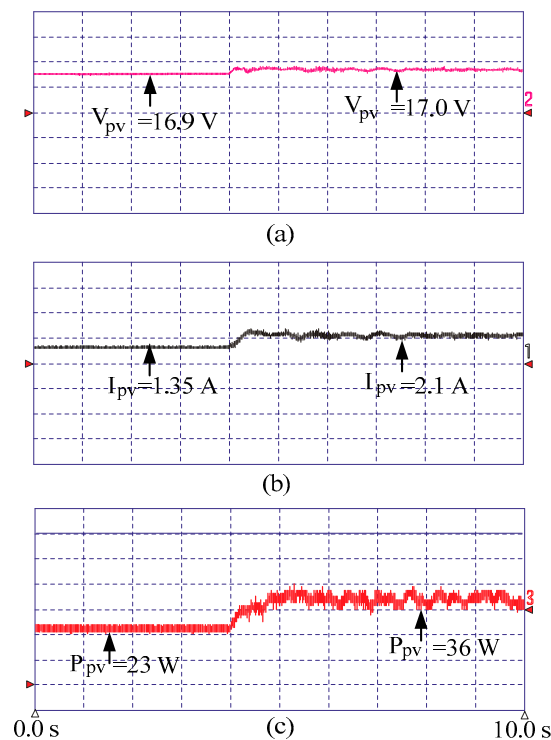


Figure 13. PV voltage, current, and power of P&O MPPT when irradiation changes (a) PV voltage, (b) PV current, (c) PV power.

The results from Figures 9–12 demonstrate the accuracy of the proposed optimization method in conducting the operation of the boost converter to GMPP, regardless of the irradiance or shading conditions of the PV system. The proposed optimization method allows for the best possible power to be generated, which guarantees the maximum energy productivity of a real PV system.

7. Conclusions

In this work, the problem related to partial shading in PV systems is overcome by using a global MPPT algorithm, implemented by using the OGWO method to maximize the extraction of energy available in PV arrangements connected to the grid. For a better understanding of the functioning of a PV panel, an equivalent circuit that behaves in a similar way was used. An equation of the equivalent circuit was used in order to observe the behavior of the panel, as well as to plot the I-V and P-V curves for different solar radiation values. It appears that there is a considerable change in the characteristic curves as a result of partial shading effects. The entire conversion system, from the photovoltaic panel to connection to the grid, is described and analyzed.

Therefore, an MPPT controller has been implemented based on the GWO optimization method so that the PV system can effectively reach GMPP. The OBL algorithm is added to the GWO to accelerate the reach of MPP by directing the search for the best solution. In order to apply the proposed solution to mirror a real operating condition as closely as possible, partial shading conditions were emulated by using semi-transparent sheets over a typical PV system.

Experimental tests of several cases of the system were conducted to better demonstrate the functioning of the OGWO-MPPT method. The algorithms also demonstrate the ability to converge to the GMPP even for abrupt variations in solar irradiance when the PV array is subjected to partial shading in the shortest convergence time, as well as the smallest power fluctuation in steady-state condition. Finally, when compared with the P&O method, it was found that the proposed method has shorter convergence time and lower fluctuations around the MPP.

Future work on this topic will be to implement the same algorithm in different topologies of PV grid-connected systems in order to assess the method performance with different topologies, as well as to test other parameters of the GWO algorithm in order to improve the dynamic performance of the proposed method.

Author Contributions: Conceptualization, A.G.A.-K. and K.S.; methodology, A.A.; validation, A.G.A.-K., N.A. and A.A.; resources, A.A.; data curation, A.G.A.-K.; writing—original draft preparation, N.A.; writing—review and editing, A.A. and N.A.; supervision, A.G.A.-K. All authors have read and agreed to the published version of the manuscript.

Funding: This research received no external funding.

Acknowledgments: The authors extend their appreciation to the Deputyship for Research and Innovation, Ministry of Education in Saudi Arabia, for funding this research work through project number (IFP-2020-03).

Conflicts of Interest: The authors declare no conflict of interest.

Nomenclature

I_{ph}	the photocurrent
I_d	the diode saturation current
A	diode ideality factor of a solar cell
V_{oc}	cell open voltage
V_{OC}	PV array open voltage
I_{sc}	cell short-circuit current
I_{SC}	PV array short-circuit current
N_s	number of series solar cells
N_p	number of parallel solar cells
I_o	diode saturation current
k	Boltzmann constant
q	charge [C]
R_{sh}	the parallel resistance
S_N	the unit solar irradiance
B	the manufacturing constant
I_t	short-circuit current temperature coefficient at surface temperature rise [A/K]
T	ambient temperature [K]
T_c	solar cell temperature [K]
T_r	solar cell reference temperature [K]
I_o	reverse saturation current [A] at solar cell operating temperature
E_g	energy band gap (Si PN junction energy gap, 1.12 [eV])

References

1. Abo-Khalil, A.G.; Berrouche, Y.; Barhoumi, E.M.; Baseer, A.M.; Praveen, R.P.; Awan, A.B. A low-cost PMSG topology and control strategy for small-scale wind power generation systems. *Int. J. Eng. Sci. Res. Technol.* **2016**, *5*, 585–592.
2. Morimoto, S.; Nakayama, H.; Sanada, M.; Takeda, Y. Sensorless output maximization control for variable-speed wind generation system using IPMSG. *IEEE Trans. Ind. Appl.* **2005**, *41*, 60–67. [[CrossRef](#)]
3. Li, H.; Chen, Z. Overview of different wind generator systems and their comparisons. *IET Renew. Power Gener.* **2008**, *2*, 123–138. [[CrossRef](#)]
4. Kim, H.S.; Lu, D.D. Review on Wind Turbine Generators and Power Electronic Converters with the Grid-Connection Issues. In Proceedings of the 2010 20th Australasian Universities Power Engineering Conference, Christchurch, New Zealand, 5–8 December 2010.
5. Abo-Khalil, A.G.; Awan, A.B. Comparative Study of Passive and Active Islanding Detection Methods for PV Grid-Connected Systems. *Sustainability* **2018**, *10*, 1798. [[CrossRef](#)]
6. Karami, N.; Moubayed, N.; Outbib, R. General review and classification of different MPPT Techniques. *Renew. Sustain. Energy Rev.* **2017**, *68*, 1–18. [[CrossRef](#)]

7. Ahmed, J.; Salam, Z. An Enhanced Adaptive P&O MPPT for Fast and Efficient Tracking under Varying Environmental Conditions. *IEEE Trans. Sustain. Energy* **2018**, *9*, 1487–1496. [[CrossRef](#)]
8. Elgendy, M.A.; Zahawi, B.; Atkinson, D. Assessment of Perturb and Observe MPPT Algorithm Implementation Techniques for PV Pumping Applications. *IEEE Trans. Sustain. Energy* **2012**, *3*, 21–33. [[CrossRef](#)]
9. Femia, N.; Petrone, G.; Spagnuolo, G.; Vitelli, M. Optimization of Perturb and Observe Maximum Power Point Tracking Method. *IEEE Trans. Power Electron.* **2005**, *20*, 963–973. [[CrossRef](#)]
10. Safari, A.; Mekhilef, S. Incremental conductance MPPT method for PV systems. In Proceedings of the 2011 24th Canadian Conference on Electrical and Computer Engineering (CCECE), Niagara Falls, ON, Canada, 8–11 May 2011; pp. 345–347.
11. Hussein, K.H.; Muta, I.; Hoshino, T.; Osakada, M. Maximum Photovoltaic Power Tracking: An Algorithm for Rapidly Changing Atmospheric Conditions. *IEE Proc. Gener. Transm. Distrib.* **1995**, *142*, 59–64. [[CrossRef](#)]
12. Abo-Khalil, A.G.; Lee, D.C.; Choi, J.W.; Kim, H.-G. Maximum Power Point Tracking Controller Connecting PV System to Grid. *J. Power Electron.* **2006**, *6*, 226–234.
13. Byunggyu, Y.U.; Abo-Khalil, A.G.; Matsui, M.; Yu, G. Sensorless Fuzzy Logic Controller for Maximum Power Point Tracking of Grid- Connected PV system. In Proceedings of the 12th International Conference on Electrical Machines and Systems ICEMS, Tokyo, Japan, 15–18 November 2009.
14. Kottas, T.L.; Boutalis, Y.S.; Karlis, A.D. New maximum power point tracker for PV arrays using fuzzy controller in close cooperation with fuzzy cognitive networks. *IEEE Trans. Energy Convers.* **2006**, *21*, 793–803. [[CrossRef](#)]
15. Al-Amoudi, A.; Zhang, L.L. Application of Radial Basis Function Networks for Solar-Array Modeling and Maximum Power-Point Prediction. *IEE Proc. Gener. Transm. Distrib.* **2000**, *147*, 310–316. [[CrossRef](#)]
16. Syafaruddin, E.; Hiyama, T. Artificial neural network-polar coordinated fuzzy controller based maximum power point tracking control under partially shaded conditions. *IET Renew. Power Gener.* **2009**, *3*, 239–253. [[CrossRef](#)]
17. Veerachary, M.; Senjyu, T.; Uezato, K. Neural-network-based maximum-power-point tracking of coupled-inductor interleaved-boost converter-supplied PV system using fuzzy controller. *IEEE Trans. Ind. Electron.* **2003**, *50*, 749–758. [[CrossRef](#)]
18. Hohm, D.P.; Ropp, M.E. Comparative study of maximum power point tracking algorithms. *Prog. Photovolt. Res. Appl.* **2003**, *11*, 47–62. [[CrossRef](#)]
19. Eltamaly, A.M.; Al-Saud, M.S.; Abo-Khalil, A.G.; Farah, H. Simulation and Experimental Validation of Fast Adaptive Particle Swarm Optimization Strategy for Photovoltaic Global Peak Tracker under Dynamic Partial Shading. *Renew. Sustain. Energy Rev.* **2020**, *124*, 109719. [[CrossRef](#)]
20. Eltamaly, A.M.; Al-Saud, M.S.; Abo-Khalil, A.G. Performance Improvement of PV Systems' Maximum Power Point Tracker Based on a Scanning PSO Particle Strategy. *Sustainability* **2020**, *12*, 1185. [[CrossRef](#)]
21. Eltamaly, A.M.; Al-Saud, M.S.; Abokhalil, A.G.; Farh, H.M. Photovoltaic maximum power point tracking under dynamic partial shading changes by novel adaptive particle swarm optimization strategy. *Trans. Inst. Meas. Control.* **2019**, *42*, 104–115. [[CrossRef](#)]
22. Eltamaly, A.M.; Al-Saud, M.S.; Abokhalil, A.G. A novel scanning bat algorithm strategy for maximum power point tracker of partially shaded photovoltaic energy systems. *Ain Shams Eng. J.* **2020**, *11*, 1093–1103. [[CrossRef](#)]
23. Eltamaly, A.M.; Al-Saud, M.S.; Abo-Khalil, A.G. A Novel Bat Algorithm Strategy for Maximum Power Point Tracker of Photovoltaic Energy Systems under Dynamic Partial Shading. *IEEE Access* **2020**, *8*, 10048–10060. [[CrossRef](#)]
24. Sundareswaran, K.; Vigneshkumar, V.; Sankar, P.; Simon, S.P.; Nayak, P.S.R.; Palani, S. Development of an Improved P&O Algorithm Assisted Through a Colony of Foraging Ants for MPPT in PV System. *IEEE Trans. Ind. Inform.* **2016**, *12*, 187–200. [[CrossRef](#)]
25. Abo-Khalil, A.G. Maximum Power Point Tracking for a PV System Using Tuned Support Vector Regression by Particle Swarm Optimization. *J. Eng. Res.* **2020**, *8*, 139–152. [[CrossRef](#)]
26. Yu, B.; Abo-Khalil, A.G.; So, J.; Yu, G. Support vector regression based maximum power point tracking for PV grid-connected system. In Proceedings of the 2009 34th IEEE Photovoltaic Specialists Conference (PVSC), Philadelphia, PA, USA, 7–12 June 2009; pp. 002037–002042.
27. Eltamaly, A.M.; Farh, H.M.H. Dynamic global maximum power point tracking of the PV systems under variant partial shading using hybrid GWO-FLC. *Sol. Energy* **2019**, *177*, 306–316. [[CrossRef](#)]

28. Abo-Khalil, A.G. Sensorless Gradient Approximation Controller for Maximum Power point Tracking of Grid Connected PV System. In Proceedings of the Middle East Power System Conference MEPCON 2015, Al Mansoura, Egypt, 15–17 December 2015.
29. Abo-Khalil, A.G.; Yu, B. Current estimation based maximum power point tracker of grid connected PV system. In Proceedings of the 2013 IEEE 10th International Conference on Power Electronics and Drive Systems (PEDS), Kitakyushu, Japan, 22–25 April 2013; pp. 948–952.
30. Abo-Khalil, A.G. Gradient Approximation Based Maximum Power Point Tracking for PV Grid Connected System. In Proceedings of the 9th Power Electronics and Drive Systems Conference PEDS, Singapore, 5–8 December 2011.
31. Wu, T.; Xu, S. A novel grey wolf optimizer for global optimization problems. In Proceedings of the 2016 IEEE Advanced Information Management, Communicates, Electronic and Automation Control Conference (IMCEC), Xi'an, China, 3–5 October 2016; pp. 1266–1270.
32. Mirjalili, S.; Mohammad, S.; Lewis, A. Grey Wolf Optimizer. *Adv. Eng. Softw.* **2014**, *69*, 46–61. [[CrossRef](#)]
33. Eltamaly, A.M.; Al-Saud, M.S.; Sayed, K.; Abo-Khalil, A.G. Sensorless Active and Reactive Control for DFIG Wind Turbines Using Opposition-Based Learning Technique. *Sustainability* **2020**, *12*, 3583. [[CrossRef](#)]

Publisher's Note: MDPI stays neutral with regard to jurisdictional claims in published maps and institutional affiliations.



© 2020 by the authors. Licensee MDPI, Basel, Switzerland. This article is an open access article distributed under the terms and conditions of the Creative Commons Attribution (CC BY) license (<http://creativecommons.org/licenses/by/4.0/>).